Multifractal Discrimination Model of High-Frequency Pupil-diameter Measurements

Bin Shi, Kevin Moloney, Virginia Emery,
Julie Jacko, Francois Sainfort and Brani Vidakovic
School of Industrial and Systems Engineering
Georgia Institute of Technology, Atlanta, GA 30332-0205, USA
(e-mail:{bshi|kmoloney|vkermery|jacko|sainfort|brani}@isye.gatech.edu)

***Abstract*— Multifractality present in high frequency pupil diameter measurements, usually connected with irregular scaling behavior and self-similarity, is modelled with statistical accuracy. A multifractal spectrum is used to discriminate pupil behavior measurements from four groups differing in ocular pathology. Broadness and the spectrum maximum, two measures characterizing the multifractal spectrum of observations, are proposed as the distinguishing features among the groups. Analysis based on descriptive statistics and kernel density estimation is provided to obtain the statistical description of the inherited mulitfractality. Model-free classification, together with the model combining technique, is adapted to build a reasonable classifier.**

I. Introduction

The discipline of human computer interaction (HCI) strives to evaluate and improve user performance and interaction with information technologies for many different users in many different contexts. Many previous investigations have examined the interactions of users with age-related macular degeneration (AMD) [*Jacko et al,* 2001], [*Jacko et al,* 2003a], [*Jacko et al,* 2003b], as it is one of the leading causes of visual impairment and blindness for individuals 55 years of age and older [*The Schepens Eye Research Institute,* 2002]. Mental workload has long been recognized as an important component of human performance during interaction with complex systems [*Gopher & Donchin,* 1986]. Notably, extreme levels of workload (high and low) have been shown predictive of performance decrements. Measures of workload can be performance-based, survey-based, or physiologically assessed.

Since the majority of information offered by computers is presented visually on a screen, these users are at a clear disadvantage. Research efforts directed towards the characterization of computer interaction for users with visual impairments can provide designers with the knowledge to better anticipate user needs in the development of information technologies. Many previous investigations have examined the interactions of users with age-related macular degeneration (AMD) [*Jacko et al,* 2001], [*Jacko et al,* 2003a], [*Jacko et al,* 2003b], as it is one of the leading causes of visual impairment and blindness for individuals 55 years of age and older [*The Schepens Eye Research Institute,* 2002].

AMD affects central, high-resolution vision, which has a large impact on the individual's ability to perform focus-intensive tasks, such as using a computer (Center for the Study of Macular Degeneration, 2002). Researchers have found that users with AMD tend to perform worse than normally-sighted users, as measured by performance metrics such as task times and errors, on simple computer-based tasks [*Jacko et al,* 2001], [*Jacko et al,* 2003a], [*Jacko et al,* 2003b]. However, little work has been done to examine how these performance decrements are affected by increases in mental workload due to sensory impairments. Mental workload has long been recognized as an important component of human performance during interaction with complex systems [*Gopher & Donchin,* 1986]. Notably, extreme levels of workload (high and low) have been shown predictive of performance decrements. Measures of workload can be performance-based, survey-based, or physiologically assessed.

Pupil diameter is a well-documented, physiological measure of mental workload (see [*Loewenfeld,* 1999] and [*Andreassi,* 2000]). While research has shown pupillary activity to be related to changes in mental workload and task difficulty in a number of domains ([*Backs,* 1992];[*Kahneman,* 1973]; [*Beatty,* 1982]; [*Marshall et al,* 2002]), the complex control mechanism of the pupil has made it difficult to extract the small, meaningful signals, related to changes in mental workload from the larger, overall noisy signal of pupillary activity [*Barbur,* 2003]. This being said, it is necessary to develop analytical techniques that can isolate these small changes in pupillary behavior. A more comprehensive analysis of the pupil signal may provide a solution to this problem and provide a unique characterization of interaction for individuals with AMD.

The development of analytical tools for high frequency data lends strong support to the analysis of the pupil signal. The high frequency pupil signal shares many important features with other extensively studied signals, such as the turbulence[*Shi et al,* 2003], internet traffic[*Abry & Veitch,* 1998] and high frequency financial time series[*Mandelbrot et al,* 1997]. This type of data are considered selfsimilar signals, which are always connected with fractals. Fractal signals are usually divided into two classes - the mono-fractal signal and the multifractal signal. Although a multifractal signal model has been applied in many other fields, no previous work has been done with pupil signals. This paper addresses the modeling of pupil signals, which are

untractable using traditional statistical models. We describe a multifractal spectra model to fit the pupil signals and then extract the signal features from this model in order to discriminate the measurements coming from the different visual acuity groups.

The dataset is described in Section II. Section III includes the description of multifractal spectrum model and the features based on the multifractal spectrum. Discriminate analysis of the pupil measurements using the multifractal model is presented in Section IV. Section V provides conclusions.

II. Pupil-diameter Measurement

In this section, we briefly describe the datasets and how the data is preprocessed to fit the further analysis.

A. Datasets description

The equipment used to collect pupillary response data during this study was the Applied Science Laboratories (ASL) Model 501 head-mounted optics systems. Pupil size was recorded, at a rate of 60 Hz, for each participant over 105 trials of a computer-based task using a graphical user interface (GUI). A camera records the pupil image, which has been illuminated by a near-infrared beam that illuminates the interior of the eye. Pupil size is assessed as the number of pixels attributed to the pupil's image, which has been determined by real-time edge detection processing of the image. Actual pupil diameter measurements (in millimeters) are then calculated by multiplying each pixel value by a scaling factor that is based on the physical distance of the camera from the participant's eye.

The dataset is comprised of pupillary response data streams for 36 individuals, as described in Table I. In this table, N refers to the number of individuals comprising this user group. Visual acuity refers to the range of visual acuity scores (assessed by ETDRS) of the better eye for participants of each group. AMD? refers to the presence (Yes) or absence (No) of this ocular disease in individuals within each group. N umber of data sets refers to the number of 2048-length data sets that were obtained from the data streams for each group.For this study, data was collected from four groups of individuals, classified by visual acuity and the presence or absence of age-related macular degeneration (AMD). Visual acuity, an individual's ability to resolve fine visual detail, was assessed via the protocol outlined in the Early Treatment of Diabetic Retinopathy Study (ETDRS) (University of Maryland School of Medicine, 1980). The experimental protocol from this study is fully described in studies by Jacko and colleagues ([*Jacko et al*, 2003a]).

TABLE I
GROUP CHARACTERIZATION SUMMARY.

Group	N	Visual Acuity	AMD?	Number of Data Sets
Control	19	20/20 - 20/40	No	111
#1	6	20/20 - 20/50	Yes	59
#2	5	20/60 - 20/100	Yes	57
#3	6	20/100	Yes	124

B. Preprocessing

Studies of pupillary response are faced with the problem of how to remove blink artifacts. A blink generally lasts about 70-100 msec (producing an artifact spanning 4-6 observations under 60 Hz sampling) during which time the camera registers loss and a pupil diameter of zero is recorded. Thus, it is generally relatively straightforward to detect and eliminate these contiguous zero observation artifacts from the record. However, on either side of a blink, one may also observe highly unusual recordings because the pupil may be measured inaccurately as the eye lid partially obscures the pupil. The result may be an impossibly small value for the pupil's size.

To insure that the analysis is conducted on pupil constriction or dilation and not on misleading discontinuities caused by blinks or partial blinks, one must either remove the blink observations from the data entirely or replace them with linearly interpolated values. Blinks (i.e., zero recordings) have been found to account for approximately 3-4% of all observations. Partial blinks account for another 1% of the total number of observations. The blink-removal procedure removes all observations having zero values (i.e., the blink) as well as any extreme values that occur within six additional observations on either side of the zero value (i.e., partial blinks).

Because of difficulty of collecting the measurements, especially from individuals with AMD, the original datasets were cut into equal length pieces to exploit their usage. Another reason of the segmentation is that the original measurements are not equally long. The segmentation is conducted after the 'Six Law' filtering, which was mentioned above. The dataset contains the sum of 351 segments of measurements after segmentation and necessary outlier detection and each have the length of 2048. The distribution of the numbers of the segments among the four groups(Control, #1, #2 and #3) is reported in the Table I.

III. Multifractality Features

In this section, we discuss the concept of multifractality and the definition of the multifractal spectrum and analyze the features of the multifractal spectrum from the perspective of discrimination.

A. Multifractal and multifractal spectrum

Many measurements encountered in nature, industry, science etc. are characterized by complex scaling behavior, namely multifractality. Multifractals are signals that, instead of a single irregularity index H (usually the worst overall index of irregularity) typical of monofractality, possess a continuous range of Hurst exponents. Prime examples of multifractals are turbulence measurements where the deviation from the constant scaling, characterized by a Hurst exponent of 1/3 and called the Kolmogorov K41 law c, is explained by multifractality of such measurements [*Mandelbrot*, 1968]. In recent years, the multifractal formalism is implemented with wavelet tools [*Arneodo,et al 1998; Reidi, 2002*]

The measure of multifractality is given by multifractal spectra that describe the "richness" of the signal in terms of various Holder regularity indices. The term spectra connotates the spectral decomposition of the signal into components characterized by their irregularity. Thus, multifractal analysis is not focused on the irregularity/self-similarity of the data set as measured by a single parameter, but rather on a measure of inhomogeneity of such a parameter.

B. Features based on multifractal spectrum

Theoretically, the multifractal spectrum of fBm (a representative of mono-fractal) consists of three geometric parts: the vertical line, the maximum point and the right slope. The maximum point corresponds to the Hurst exponent and the vertical line is thought to be an inherent feature, which distinguishes fBm from the multifractal process. However, it is rare to obtain such a perfect spectrum in practice. Even for the simulated fBm, due to error of estimation, its spectrum may deviate from the theoretical form, as shown in Figure 1. Even with the lack of precise estimation of the spectrum, the deviation from the vertical line could be still utilized in the discrimination between the mono- and multi-fractal processes. In Figure 1, two type processes are presented in the multifractal spectra. One is the fBm and the other is the turbulence measurement, which is widely believed to be a multifractal process. Comparing with the turbulence measurement, the fBm is much closer to the vertical line and this closeness may be quantified by the left slope of the spectra. Another important difference between these two spectra is the width spread of the spectra. It is obvious that the width spread of the fBm is much smaller than the turbulence measurement.

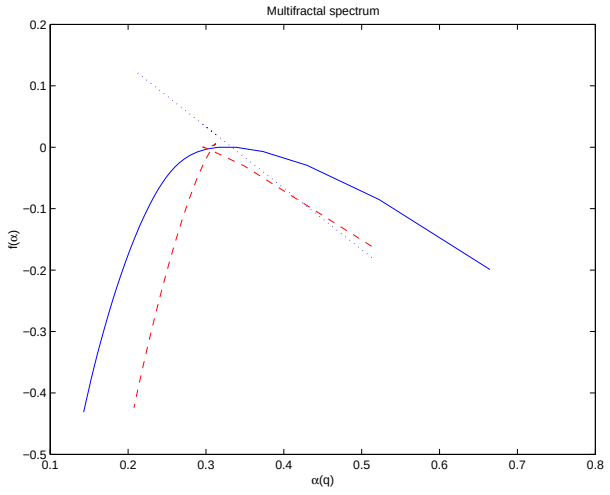

Fig. 1. Multifractal Spectra for mono- (dash line) and multi-fractal (solid line) processes (The dotted line indicates the theoretical slope of the spectrum for monofractal process)

Despite the existence of the estimation error, the spectrum can be approximately described by two slopes and one point without loss of the discriminant information. Alternatively, we can also approximate the spectrum by the left slope, the maximum point and the width spread. A typical multifractal spectrum is described as shown in Figure 2.

The left and right slopes can be obtained easily using the linear regression technique. However, it is not as straightforward to define the width spread automatically. The difficulties are related to two aspects - one being how to locate the start and end points of the width spread, while the other is what to do with the discreteness of the spectrum. It is easy to see that the former is difficult conceptually, while the latter is computationally difficult. There are many ways to define the width spread. In this paper, we give one definition of width spread and we name the width spread the *broadness* of the spectrum.

Definition Suppose that α_1 and α_2 are two roots which satisfy the equation $f(\alpha)+0.2=0$ and $\alpha_1 < \alpha_2$, the the broadness of multifractal spectrum is defined as $B = \alpha_2 - \alpha_1$, where $f(\alpha)$ is the spectrum function in terms of Holder regularity indices α's.

This definition is also graphically presented in Figure 2. The deviation from the mono-fractal could be fairly compared according to this Broadness measure since it posts a universal standard on the width spread. It is worth to point out the threshold value 0.2 used in this definition could be adjusted empirically in the practice analysis to insure that this measure is well defined for all analyzed signals.

As mentioned earlier, the discreteness may produce difficulties in the computation. The problem is that it may be hard to find the exact roots of the equation $f(\alpha)+0.2=0$ among the discrete values of α's. To get around this, we try to find the minimum value of $|f(\alpha)+0.2|$ with respect of α instead of solving the equation directly.

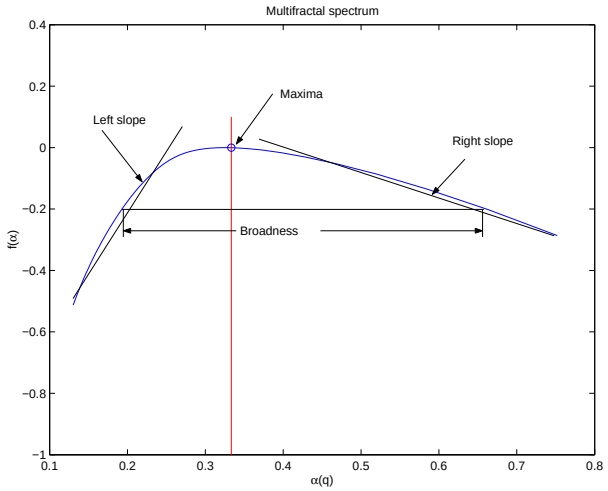

Fig. 2. Approximate description of the spectral characteristics

IV. Pupillary Responses Analysis

As mentioned previously, we attempt to find the inherent features which can separate the types of measurements from each other. The empirical evidence has shown that Pupil-diameter measurements possess self-similarity and fractality. Hence, it is natural to apply the multifractal spectra to discriminate these measurements.

We have discussed the features of multifractal spectra in section **??**. The most important feature of the spectra is the maximum point, which corresponds to the Hurst exponent. The Hurst exponent is a measure of "roughness"of the self-similar process.The Hurst exponent coincides with the Holder regularity index, and signals with H close to 0 look quite irregular and intermittent while for H close to 1, the signals look smooth. Such an important property of the Hurst exponent enables us to explain the dynamics of pupillary behavior. Informally speaking, large values of Hurst exponent correspond to low dynamic in the change of pupil size ("frozen eye") while low values of the exponent indicate bursty and frequent changes. Therefore, the Hurst exponent could discriminate the measurements. The boxplots of the Hurst exponents for the four groups are shown in Figure IV. According to this figure, the second group(#1) have exponents much lower than the control group, which reflects that the individuals from this group have more irregular pupillary responses than those from the control group.

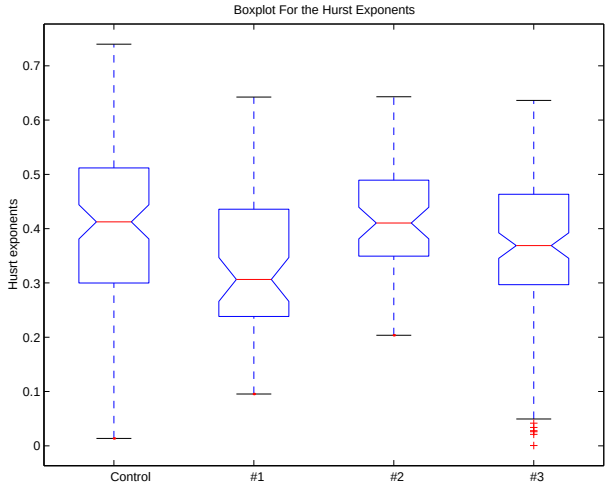

Fig. 3. Boxplot for the Hurst exponent of multifractality.

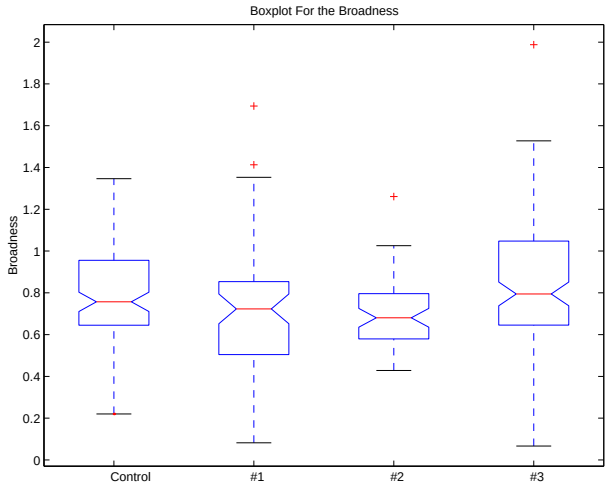

Fig. 4. Boxplot for the Broadness measure of multifractality.

As can be seen in Figure IV(Left), the Hurst exponent could not completely discriminate the groups. This motivates us to introduce other discriminatory quantities. Another measure we just defined is the broadness, which is able to distinguish the deviation from monofractality. Broadness describes richness in the distribution of the Hurst exponent. Pupil-diameter measurements with narrow multifractal spectra are close to monofractals (i.e., the scaling is quite uniform over all scales). The boxplot of the broadness are given in Figure IV. It is very hard to tell the difference among the four groups. However, the last group(#3) significantly differs in terms of the broadness from other experimental groups(#1, #2). Group #3 has relatively high large broadness measure, which indicates that the pupillary responses of the individuals from this group deviates from monofractal much more than groups #1 and #2.

Neither the Hurst exponent nor the Broadness measure are able to achieve the complete discrimination separately. Thus, we need to increase the analysis into the 2D plane, analyzing the data with both measures simultaneously. Figure 5 presents the centroid points for the four groups. These four points look nearly evenly distributed on the plane. From this figure, we can see that the Hurst exponent from the control group is relatively large although it is not the largest. There is only one group (group #2), which has bigger Hurst exponent than the control group. Comparing these two groups, we can tell that the Pupil-diameter measurement from the control group is further from monofractal than group #2 since the broadness measure of group #2 is the smallest.Therefore, we can claim that the pupillary responses of individuals from the control group is very smooth but fractal properties are relatively inhomogeneous, which implies the causes of the regularity are quite rich. Group #1 is located on the very left-bottom side of the plane and hence it represents as measurements with much irregular dynamics and homogeneous fractal properties (indicates the cause of the irregularity is relatively simple). Group #3 located on the top, close to the left side signifies that the measurements are quite irregular and have inhomogeneous fractal properties(indicates the cause of the irregularity is not single).

To further address how the Hurst exponent and Broadness could be the discriminating measures, we estimate bivariate kernel densities of them for each group. The contours of these densities are given in the Figure 6. This figure includes all the information shown in Figure 5. The variability information of the two measures within each group, however, provides more discriminating features. It is easy to see that measures in group #2 are very compact while those in group #3 are dispersed.

Another important task in the analysis of these measurements is classifier training. Among the many candidates, the k-nearest-neighbor classifier is chosen because it is model free. The original datasets are divided into two parts, one of them is assigned to training set and the other is used to test the trained classifier. The training set includes 90% randomly selected sample of each group from the whole datasets and the rest is taken to be the test setTo choose the nearest neighbor parameter k, the classifier is built as a learning process. The

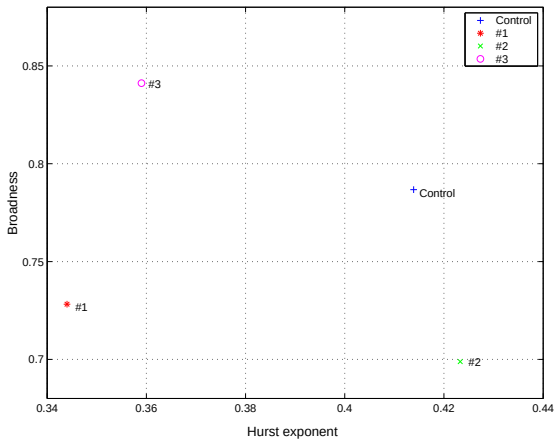

Fig. 5. Centroid points from bivariate measures:Hurst exponent and Broadness

learning curve, which includes the test error and training error corresponding to different parameters k, is given in Figure IV. Although, relatively low training error could be achieved by choosing small k, the test error is too big for a practically useful classifier. To overcome these drawbacks, we adapt the model by combining techniques. Model combining is a technique of combining the predictions from different classifiers. The results have shown to be promising. For the details of this combining technique, the reader is referred to [*Xu et al*, 1992]. The advantage of using model combining is due to its ability of overcoming the instability of the single classifier. In our study, the single k-nearest-neighbor classifier is not very accurate and robust according to Figure IV. By applying the model combining technique to these k-nearest-neighbor classifiers ($3 \leq k \leq 10$), the test errors get much smaller as we can see from Table II. Although the combining rules do not make much difference, the result from mean-combining rule is shown to be optimal among the alternatives. Up to now, all analysis is done according to two features: the Hurst exponent and Broadness. To demonstrate how an additional measure may affect the classifier quality, we add the left slopes into the feature vectors and the result of classification design is reported in Table III. It is apparent that both the test and training errors decrease a lot as the new feature is added (e.g. the test errors drops down about 6%).

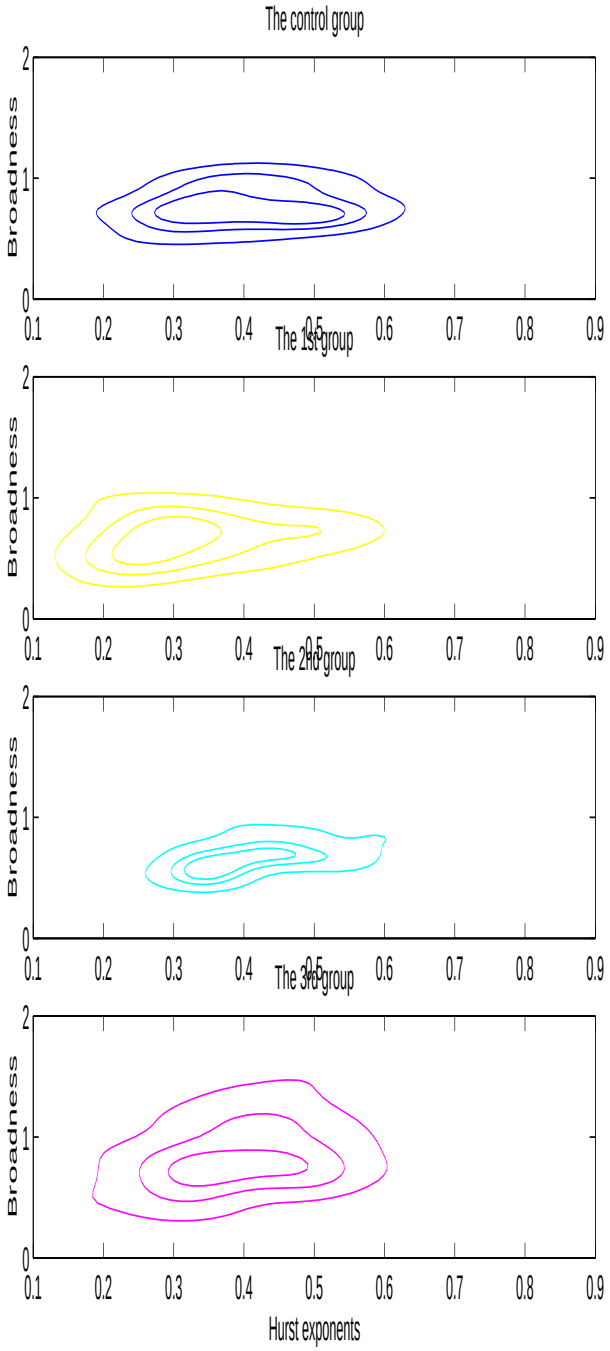

Fig. 6. Joint density of both the Hurst exponent and Broadness

V. Conclusions

The overreaching goal of this detailed analysis was to determine if individuals with different visual abilities exhibit quantifiable differences in their interaction with graphical user interfaces. These distinctions between classes of users can enable developers to design improved interfaces for more efficient and effective human-computer interactions. Pupillary behavior is an informative, yet complex, means of quantifiably assessing differences in the interaction behaviors of users.

Measurements of pupil diameter during task performance is one way to study the effects of mental workload on users. However, the inherent complexity of pupillary behavior requires that robust and valid measures be developed to extract the meaningful components of the data stream in order to characterize those changes in pupillary behavior that distinguish changes in mental workload. In this way, the relative mental workload of users with different visual capabilities can be examined. These distinctions between user needs can be used to modify visual interfaces and interaction paradigms in order to best adapt information technologies for users with visual impairments.

In this paper, we study how to incorporate characteristics of the multifractal spectrum into the modeling and discrimination of the Pupil-diameter high frequency measurement.

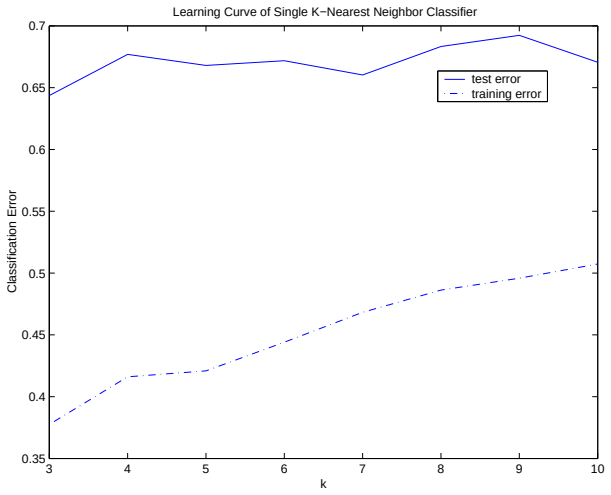

Fig. 7. Learning Curve of K-Nearest Neighbor Classifier

TABLE II

ERROR RATE AFTER COMBINING THE NEAREST NEIGHBOR CLASSIFIERS

	rule	mean	median	max	min	majority voting
Training	mean	0.42	0.43	0.44	0.42	0.46
Errors	std. dev.	0.01	0.01	0.02	0.02	0.01
Test	mean	0.51	0.53	0.52	0.52	0.55
Errors	std. dev.	0.09	0.07	0.08	0.09	0.07

TABLE III

ERROR RATE AFTER COMBINING THE NEAREST NEIGHBOR CLASSIFIERS(ADDING SLOPE FEATURE)

	rule	mean	median	max	min	majority voting
Training	mean	0.407	0.414	0.417	0.401	0.432
Errors	std. dev.	0.013	0.012	0.015	0.015	0.013
Test	mean	0.446	0.450	0.439	0.459	0.475
Errors	std. dev.	0.051	0.045	0.048	0.057	0.050

The multifractal process was validated to be appropriate in the analysis of the Pupil-diameter measurements. By decomposing the spectrum into describable parts, the feature extraction is discussed to do further discrimination. The concept of the Broadness of a multifractal spectrum is defined. The analysis based on the Hurst exponent and Broadness measures gave distinguishable characteristics of the pupillary responses from the individuals with different visual acuity ranges. The model-free classification method, k-nearest-neighbor classifier, is applied with the model combining technique to build a reasonable classifier.

REFERENCES

[*Abry & Veitch*, 1998] Abry &Veitch(1998),Wavlet analysis of long rang depedent traffic,*IEEE Trsanctions on Information Theory*, 44:2-15, 1998

[*Andreassi*, 2000] Andreassi, J. L. (2000). Psychophysiology: Human behavior & physiological response (4th ed.). Mahwah, NJ: Lawrence Erlbaum Associates.

[*Backs*, 1992] Backs, R.W. & Walrath, L.C. (1992). Eye movement and pupillary response indices of mental workload during visual search of symbolic displays. Applied Ergonomics, 23, 243-254.

[*Barbur*, 2003] Barbur, J. L. (2003) Learning from the pupil - studies of basic measurement mechanisms and clinical applications. L. M. Chalupa & J.S. Werner (Eds.), Cambridge, MA: MIT Press, in press.

[*Beatty*, 1982] Beatty, J. (1982) Task-evoked pupillary responses, processing load, and the structure of processing resources. Psychological Bulletin, 91, 377-381.

[*Beran*, 1994] Beran, J., Statistics for Long Memory Processes, New York: Champan & Hall, 1994

[*Coeurjolly*, 2000] Coeurjolly,J.F.(2000), Simulation and identification of the fractional Brownian motion: a bibliographical and comparative study *JSS* 07,2000

[*Gopher & Donchin*, 1986] Gopher, D., & Donchin, E. (1986). Workload-An Examination of the Concept. In K. R. Boff, L. Kaufman, & J. P. Thomas (Eds.), *Handbook of Perception and Human Performance* (pp. 41-1 - 41-49). New York, NY: John Wiley and Sons.

[*Hastie, et al*, 1996] Hastie, T. and Tibshirani, R.(1996) Discriminant Analysis by Gasssian mixtures, *J. Royal. Statist. Soc. B* 58:155-176.

[*Hurst*, 1951] Hurst, H. E.(1951), Long-Term Storage Capacity of Reservoirs., *Proc. American Society of Civil Eng.*, 76(11), 1950.

[*Jacko et al*, 2001] Jacko, J. A., Scott, I. U. , Barreto, A. B., Bautsch, H. S., Chu, J. Y. M., & Fain, W. B.(2001) Iconic visual search strategies: A comparison of computer users with AMD versus computer users with normal vision. *Proceedings of the 9th International Conference on Human-Computer Interaction*, New Orleans , LA, August 5-10, 423 -427.

[*Jacko et al*, 2002] Jacko, J. A., Barreto, A. B., Scott, I. U., Chu, J. Y. M., Vitense, H. S., Conway, F. T., & Fain, W. B. (2002). Macular degeneration and visual icon use: deriving guidelines for improved access. *Universal Access in the Information Society*, 1(3), 197-206.

[*Jacko et al*, 2003a] Jacko, J. A., Scott, I. U., Sainfort, F., Barnard, L., Edwards, P. J., Emery, V. K., Kongnakorn, T., Moloney, K. P., & Zorich, B. S. (2003a). Older adults and visual impairment: What do exposure times and accuracy tell us about performance gains associated with multimodal feedback? *CHI Letters*, 5(1), 33-40.

[*Jacko et al*, 2003b] Jacko, J. A., Scott, I. U., Sainfort, F., Moloney, K. P., Kongnako, T., Zorich, B. S., & Emery, V. K. (2003b). Effects of multimodal feedback on the performance of older adults with normal and impaired vision. *Lecture Notes in Computer Science (LNCS)*, 2615, 3-22.

[*Kahneman*, 1973] Kahneman, D. (1973). Attention and effort. Englewood Cliffs, NJ: Prentice-Hall.

[*Loewenfeld*, 1999] Loewenfeld, I. E. (1999). The pupil: Anatomy, physiology, and clinical applications (2nd ed.). Oxford, UK: Butterworth-Heinemann.

[*Mandelbrot*, 1968] Madndelbrot, B. et al(1968), Fractional Brownian Motion, Fractional Noise and Applications, *SIAM review*, 10, 422-437, 1968

[*Mandelbrot et al*, 1997] Mandelbrot, B.B., Calvet, L., Fisher, A.(1997), A Multifractal Model of Asset Returns. Working Paper. Yale University. Cowles Foundation Discussion Paper #1164.

[*Marshall et al*, 2002] Marshall, S. P., Pleydell-Pearce, C. W., & Dickson, B. T. (2002). Integrating psychophysiological measures of cognitive workload and eye movements to detect strategy shifts, In Proceedings of the 36th Hawaii International Conference on System Sciences (HICSS '03).

[*Shi et al*, 2003] Shi, B., Vidakovic, B., Katul, G. and Albertson, J.(2003), "Assessing the Effects of Atmospheric Stability on Inertial Subrange Turbulence using Multiscale Approaches", Working paper, ISyE, Georgia Tech.

[*The Center for the Study of Macular Degeneration*, 2002] The Center for the Study of Macular Degeneration, University of California, Santa Barbara. (2002, January 25). Biology of AMD. Retrieved October 15, 2002, from http://www.csmd.ucsb.edu/faq/faq.html

[*The Schepens Eye Research Institute*, 2002] The Schepens Eye Research Institute, Harvard Medical School, Harvard University. Macular degeneration: Your questions answered. Retrieved November 12, 2002, from http://www.eri.harvard.edu/htmlfiles/md.html

[*Xu et al*, 1992] Xu, L., Krzyzak, A., and Suen, C.Y. (1992), Methods of combining multiple classifiers and their application to handwriting recognition, *IEEE Trans. SMC*, 22, 1992, 418–435.